ORIGINAL PAPER

Precise estimation of horizontal displacement by combination of multi-GNSS (Galileo and GPS) observations via the LS-VCE method

Saeed Farzaneh[1] · Abdolreza Safari[1] · Kamal Parvazi[1]

Abstract

In the present study, the role of the stochastic model in processing GNSS observations and determining the horizontal displacement parameters is investigated. Stochastic modeling has been evaluated using two approaches; (1) nominal weight and (2) estimated weight. The former is based on the experimental fixed values, meanwhile the latter is based on the least-square variance components estimation (LS-VCE) method, which is implemented for GNSS observations to estimate the components of variance of observations directly. In this research showed that the stochastic model plays an important role in detecting small displacements. For this purpose, a high-precision displacement simulator which can move accurately at short distances in one direction as well as on a horizontal plane was used. A simulated displacement motion experiment was performed. Derived displacements were compared with simulated (real) displacements along with their accuracy in two modes using only GPS and multi-GNSS as well as the two weighting modes provided. The results of the coordinate comparison show that the stochastic model based on the LS-VCE in the PPP method gives a difference of 0 and -1.9 mm for the east–west and north–south components, while the use of nominal weight, a difference of -1.9 and -1.1 mm. Also, the maximum accuracy improvement in this case for these two coordinate components is 7.8 and 4 mm, respectively, also considering the combination of multi-GNSS observations, the accuracy of the coordinate components and the horizontal component in the weight estimation model has provided an improvement of 5.8 and 5.3 mm. In general, the combination of observations has increased the accuracy of the displacement component compared to the single system.

Keywords Deformation monitoring · Precise point positioning (PPP) · Variance component estimation (VCE) · Least squares estimation (LSE) · Multi-GNSS

Introduction

Monitoring the deformation of engineering structures is an important approach to presenting the necessary measures to prevent economic and financial damage. For this reason, it is necessary to analyze deformation in different structures. The monitoring and analysis of deformation in various structures are a special branch of geodesy. There are several techniques

✉ Saeed Farzaneh
  farzaneh@ut.ac.ir

  Abdolreza Safari
  asafari@ut.ac.ir

  Kamal Parvazi
  kamal.parvazi@ut.ac.ir

[1] School of Surveying and Geospatial Engineering, College of Engineering, University of Tehran, North Kargar Street, 149957131 Tehran, Iran

to measure deformation, which are divided into two main groups, namely geodetic and non-geodetic ones. Each one has its advantages and disadvantages. Geodetic techniques allow for the analysis of deformation, as well as statistical tests by considering the network of points and observations of length, angle, height difference, direction, azimuth, and so on. Today, global navigation satellite systems (GNSS) technology is used in many types of research and industrial fields due to the position accuracy, observation availability, and development of processing algorithms (Yigit et al. 2016).

Two GNSS positioning methods tend to be used to achieve the accuracy required to monitor deformations (Xu et al. 2011; Capilla et al. 2016; Erol and Ayan 2003). Each of these two methods has advantages and disadvantages. The relative method requires two or more receivers, while the precise point positioning (PPP) method is a cost-effective method that uses only one receiver. This method provides displacements according to a global reference framework.

The relative positioning method provides more accurate results. This is especially the case in short baselines, where all common factors such as the satellite and receiver clock, atmospheric delays, are eliminated or reduced significantly by the double differencing model. One of the disadvantages of this technique, widely accepted for precise geodetic and geophysical purposes, is the need for simultaneous observations in known and unknown stations. Also in this method, the accuracy of measurements depends on the length of the baseline and the duration of observation (Paziewski et al. 2018; Yigit et al. 2016; Hofmann-Wellenhof et al. 2007; Alcay et al. 2019; Fermi et al. 2019; Dabove et al. 2020). However, due to advances such as increasing the constellation and augmenting the number of signals with the integer ambiguity resolution, the limitations of the PPP method such as longer convergence time and its accuracy can be improved (Ge et al. 2008; Dabove et al. 2014). In the relative approach, 1–2 mm for the horizontal component and 3–5 mm for the vertical component have been presented by Firuzabadı` and King 2012 (provided that four reference stations are utilized). It will also be possible for the PPP method to achieve an accuracy of 5 mm should the daily observations be used (Gandolfi et al. 2017). Therefore, both methods are used for different deformation monitoring applications. The PPP method is used in numerous applications such as the earth surface changes (Poluzzi et al. 2020; Hu et al. 2014; Martín et al. 2015; Dabove et al. 2014), detecting of structures displacement (Yigit 2016; Roberts et al. 2019), tectonic and geophysical studies (Geng et al. 2017), detecting of earth subsidence (Chatterjee et al. 2015), and GPS buoy (Savage et al. 2004; Hammond and Thatcher 2005; Fund et al. 2013).

One of the important factors in achieving high-quality results in the PPP method is choosing the appropriate method for processing observations. Each processing method consists of two functional models and a stochastic model that must be properly modeled. In the PPP method, an ionospheric-free (IF) linear combination is generally used as a functional model. In the ionospheric-free model, how to deal with errors is very important. Many factors cause errors in this model. These factors include the limited accuracy of the satellite orbit and clock products, the effect of the residual errors that have not been modeled, and the effect of the utilized stochastic model (in fact, the quality of observations depends on various effects that affect the accuracy of the observation. This is related to the signal propagation and the quality of the receiver). The ability to estimate phase ambiguity as an integer will also be effective in providing PPP accuracy, particularly for the east component. Concerning other parameters such as a reduction in the convergence period in the PPP method, several factors such as the number and geometry of the observed satellites (this factor can also improve the quality of the zenith tropospheric delay parameter), environment and dynamics of the receiver used,

quality of observations, sampling rate, and stochastic model are effective. By changing these factors, the two parameters of accuracy and convergence time will change. Reducing all errors in the PPP performance is necessary to achieve results with better accuracy. In general, by modeling errors (troposphere, relativity, satellite antenna PCO/PCV, solid earth tide, phase windup, ocean loading, satellite orbits/clocks, receiver antenna PCO/PCV), filtering the effect of pseudo-range multipath and noise and using the ionosphere-free linear combination to eliminate the ionosphere effect, high accuracy can be achieved in the PPP method (Abou-Galala et al. 2018; Karimi 2021; Kouba et al. 2017; Marreiros et al. 2012; Ge et al. 2008; Héroux et al. 2004; Bisnath and Gao 2009; Beran 2008; Lou et al. 2014).

In association with the stochastic model, it is noted that this model has high importance in estimating unknown parameters since the minimum variance estimators can be achieved in a linear model providing that the weight matrix is selected as the inverse of the covariance matrix of the observables (Koch 1999; Li et al. 2010). On the other hand, in most cases, the empirical stochastic models are used for GNSS observations. Estimating the weight matrix using the available empirical stochastic models is not valid for different types of GNSS receivers and signals. These models cannot present the real accuracy for all signals due to a variety of signals sent from satellites and the development of satellite navigation systems. This is because the observations of satellite systems have different quality. One of the reasons for the difference in their quality is the noise level of the observations (Quan et al. 2016; Afifi and El-Rabbany, 2013). Due to the importance of displacement monitoring using GNSS observations, several studies have been performed in this field. Among these researches, we can refer to Larson (2009), Avallone et al. (2011), and Zangeneh-Nejad et al. (2017) in which the GPS is used to study the displacements caused by earthquakes, volcanoes, and tsunamis. In researches (Nickitopoulou et al. 2006; Tang et al. 2017; Yu et al. 2014), the GNSS system is used to monitor various structures, as well as create displacement, also in studies (Eueler and Goad 1991; Gerdan 1995; Jin and de Jong 1996) the effect of variance of elevation-dependent observations was studied and based on that the variance parameter can affect the quality of the presented results. This effect was investigated in research (Amiri-Simkooei et al. 2013; Zangeneh-Nejad et al. 2015; Li 2016; Amiri-Simkooei et al. 2009) and based on the results presented in these researches and similar researches, the accuracy of the coordinate components and the convergence time parameter are influenced by the selected stochastic model.

Considering that nominal accuracy is usually used for code and phase observations, and considering the fixed numerical values for these two parameters and using the error propagation law, the accuracy of IF observations is

calculated. Therefore, in this study, one of the objectives is to estimate the variance components for ionosphere-free observations using the LS-VCE method instead of using experimental fixed values. This is because the accuracy of these parameters is different for the signals of each satellite system. On the other hand, there is usually a constant ratio between the accuracy of the code observations and the phase of the GPS with other satellite systems, which does not meet the optimal accuracy in all conditions. Therefore, in this study, using multi-GNSS observations, by directly including the observations of each system, the code and phase variance components are estimated simultaneously by the LS-VCE method and are used to detect displacement. Finally, the main purpose of the research was to investigate the effect of the estimated stochastic model in determining and measuring horizontal displacement using the PPP method. Horizontal displacement was also determined using GPS and multi-GNSS observations. It was investigated that in the PPP mode and using only one receiver in a short time, improving the stochastic model can be effective in determining small displacements. The contents of this research are as follows: at first, presents the stochastic and functional model in IF multi-GNSS PPP, as well as a complete description of the LS-VCE method. Then, presents the approach used to determine horizontal displacement, as well as statistical tests for the horizontal displacement significance test. In the following, the effect of the stochastic model on the quality of results provided by PPP is investigated, as well as the test used to detect the minimum displacement using the PPP method. Finally, the conclusions have been presented.

Multi-constellation PPP observation model

The PPP method is a satellite positioning technique, which uses two-frequency observations of code and phase from a receiver, along with satellite precise ephemeris (clock and orbit products) to determine the exact position of the receiver. In the PPP method, many errors from different sources such as troposphere delay, ionosphere delay, clock receiver, multi-path, and measured noise must be carefully handled to achieve high-quality results. In this way, the ionospheric-free composition is usually used with the help of two-frequency measurements to eliminate the effect of the ionosphere. Other parameters such as tropospheric delay and receiver clock offset are estimated simultaneously with the station coordinates. Other sources of error such as relativistic, phase wind-up, ocean loading, phase center offset (PCO), and phase center variation (PCV) receivers and satellites, and earth tides can be corrected through existing models. After eliminating, estimating, and modeling the presented errors, the first part of the mathematical model (functional model) can be carefully determined. Then, the second part of the mathematical model

(stochastic model) must also be considered. Now, by choosing a suitable processing method, we can expect that the PPP method can provide results with the desired quality (Kouba and Héroux 2001; Li and Zhang 2012). Figure 1 shows the flowchart of the proposed method.

According to this diagram, first, the model inputs including station information (RINEX observation and Differential Code Bias (https://cddis.nasa.gov/archive/gnss/products/bias/2017/)) and satellite precise ephemeris (Orbit and Clock (https://cddis.nasa.gov/archive/gnss/products/mgex/1982), and as well as Phase Center Offset (http://www.epncb.oma.be/ftp/station/general/old_calibrations/) are prepared. Corrections such as Cycle Slip Detection (Melbourne 1985), Phase Wind up (Wu et al. 1992), Solid Earth Tide, Ocean Tide Loading, and Earth Rotation (Kouba and Héroux 2001; Bisnath and Gao 2009) are then applied to the observations, then a functional model is constructed using an ionospheric-free compound; to complete the functional model, a suitable stochastic model must be considered. In this research two approaches are used to implement the stochastic model. In the first approach, the stochastic model is considered based on nominal weight and experimental variance for observations. In the second approach, a stochastic model is constructed based on the LSVCE method. Finally, with two accurate models (functional model and Stochastic model), the RLS method is used to solve PPP and estimate unknowns. These unknowns include station coordinates, clock receiver error, phase ambiguity, tropospheric delay, and time offset between the two systems.

Functional model of multi-GNSS PPP

PPP contains dual frequency measurements of one receiver along with precise products of satellite clock and orbit. Since in this research, a combination of observations of GPS and Galileo systems has been used. The IF equations for this combination for code and phase observations are as follows (Cai and Gao 2013; Cai et al. 2015; Li et al. 2018):
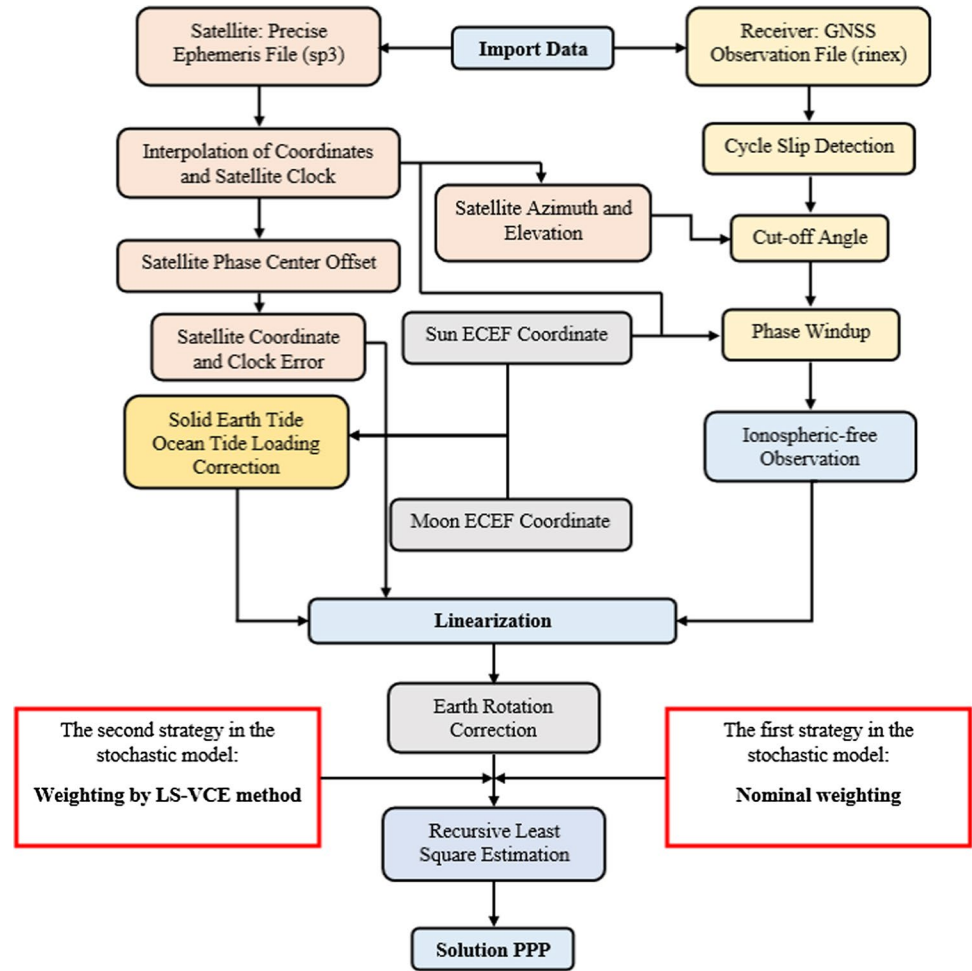
For code observation:

$$
\begin{aligned}
P_{\mathrm{IF}}^{G} &= \rho^{G} + cdt^{G} + T^{G} + \varepsilon\left(P_{\mathrm{IF}}^{G}\right) \\
P_{\mathrm{IF}}^{E} &= \rho^{E} + cdt^{G} + T^{E} + cdt_{sys}^{E} + \varepsilon\left(P_{\mathrm{IF}}^{E}\right)
\end{aligned}
\tag{1}
$$

For phase observation:

$$
\begin{aligned}
\Phi_{\mathrm{IF}}^{G} &= \rho^{G} + cdt^{G} + T^{E} + \lambda_{\mathrm{IF}}^{G} N_{\mathrm{IF}}^{G} + \varepsilon\left(\Phi_{\mathrm{IF}}^{G}\right) \\
\Phi_{\mathrm{IF}}^{E} &= \rho^{E} + cdt^{G} + T^{E} + \lambda_{\mathrm{IF}}^{E} N_{\mathrm{IF}}^{E} + cdt_{sys}^{E} + \varepsilon\left(\Phi_{\mathrm{IF}}^{E}\right)
\end{aligned}
\tag{2}
$$

In Eq. (1) and Eq. (2), $P_{\mathrm{IF}} = \alpha_{\mathrm{IF}} P_1 + \beta_{\mathrm{IF}} P_2$ and $\Phi_{\mathrm{IF}} = \alpha_{\mathrm{IF}} \Phi_1 + \beta_{\mathrm{IF}} \Phi_2$ are IF code and phase observations,

Fig. 1 Algorithm for formation of PPP

respectively, $\alpha_{\text{IF}} = \frac{f_1^2}{f_1^2 - f_2^2}$ and $\beta_{\text{IF}} = \frac{-f_2^2}{f_1^2 - f_2^2}$, $N = \frac{\lambda_1 f_1^2}{f_1^2 - f_2^2} N_1 - \frac{\lambda_2 f_2^2}{f_1^2 - f_2^2} N_2$, and f_1, f_2 the frequencies of the two signals are used. P_1, P_2 and Φ_1, Φ_2 are the pseudo-range code observations and the phase observation, respectively. ρ is the geometric distance between the receiver and the satellite, T is a tropospheric delay, dt is receiver clock, c is the speed of light, N is the correct phase ambiguity and λ wavelength, and ε represents other errors such as observation noise, receiver and satellite code, and phase hardware bias. In equations, a new parameter called cdt_{sys}^E is added to the model to indicate the time difference between GPS time system relative to Galileo.

Formulation of the stochastic model

Many stochastic models have been proposed to weight GNSS observations that are mostly derived empirically. In most of available models, only the altitude angle of satellites is considered for predefining the weights (Li 2016). However, in reality, the statistical conditions governing the observations

cannot be fully modeled because they change during the observation period (Wang et al. 2002; Roberts et al. 2019). Therefore, we propose to re-estimate these weights using a VCE algorithm. In the following, we describe the nominal weighting method and the use of experimental models, and then the weight estimation method using the LS-VCE is presented.

Nominal weight

in the nominal weight, using the error propagation law, the IF observation covariance matrix can be introduced for code and phase observations as follows (Guo et al. 2021; Rebeyrol et al. 2007; Li and Geng 2019):

$$Q = \begin{bmatrix} \sigma_{P_3}^2 & 0 \\ 0 & \sigma_{\Phi_3}^2 \end{bmatrix} Q_E, \begin{bmatrix} \sigma_{P_3}^2 & 0 \\ 0 & \sigma_{\Phi_3}^2 \end{bmatrix} = J \begin{bmatrix} \sigma_{P_1}^2 & 0 & 0 & 0 \\ 0 & \sigma_{P_2}^2 & 0 & 0 \\ 0 & 0 & \sigma_{\Phi_1}^2 & 0 \\ 0 & 0 & 0 & \sigma_{\Phi_2}^2 \end{bmatrix} J^T, J = \begin{bmatrix} \alpha_{IF} & \beta_{IF} & 0 & 0 \\ 0 & 0 & \alpha_{IF} & \beta_{IF} \end{bmatrix}$$

(3)

In Eq. (3), $\sigma_{\Phi_1}^2$ and $\sigma_{\Phi_2}^2$ are the nominal precision of phase observations, $\sigma_{P_1}^2$ and $\sigma_{P_2}^2$ are the nominal precision of code

observations, $\sigma_{\Phi_3}^2$ and $\sigma_{P_2}^2$ are the precision of the IF phase and code observations, Q_E is the elevation-dependent model which can be expressed using relationships $Q_1 = \frac{1}{sin(E)}, Q_2 = \frac{1}{sin^2(E)}, Q_3 = cos(E), Q_4 = cos^2(E)$ and $Q_5 = exp\left(\frac{-E}{E_0}\right)$, and J is the Jacobian matrix. It is assumed that P_1 and P_2 as well as Φ_1 and Φ_2 have the same accuracy. E is the satellites elevation angle(Units: degree) and $E_0 = 20$ (the constant empirical value) for IF observations (Han 1997; Gao et al. 2011).

LS-VCE weights

In this method, the accuracy of code and phase observations are estimated and used in the construction of weight matrices. There are many methods for estimating variance components. These methods include MINQUE, BIQUE, Helmert, REML, and LS-VCE. In this research, the LSVCE method has been used. This method was first introduced by Teunissen in 1988 (Teunissen 1988). It was then developed in 2007 by Amiri-Simkooei. This method considers a set of unbiased estimators that have the property of independence from the observation distribution function. Since this method follows the principle of least squares, it is easily possible to do various statistical tests (Amiri-Simkooei 2007, 2013; Amiri-Simkooei et al. 2009). The model used for the observation equations is as follows:

$$\begin{aligned} E(y) &= Ax \\ D(\text{y}) &= Q_y = Q_0 + \sum_{k=1}^{p} \sigma_k Q_k \end{aligned} \tag{4}$$

where E is the mathematical expectation; D are dispersion operators; A, y, and x are design matrix, observations vector, and unknown vector; Q_0 is the known part of covariance matrix, σ_k is variance of unknown unit weight, Q_y is covariance matrix of observations, and $Q_k, (k = 1, 2, \dots, p)$ are known co-factor matrices of models. The LS-VCE equation in linear model is presented as follows:

$$\begin{aligned} \hat{\sigma} &= N^{-1}l \\ N = n_{ij} &= \tfrac{1}{2}tr(Q_i Q_y^{-1} P_A^\perp Q_j Q_y^{-1} P_A^\perp) \\ l = l_i &= \tfrac{1}{2}\hat{e}^T Q_y^{-1} Q_i Q_y^{-1}\hat{e} - \tfrac{1}{2}tr(Q_0 Q_y^{-1} P_A^\perp Q_y^{-1} P_A^\perp) \\ P_A^\perp &= I - A^{(A^T A^T Q_y^{-1}} \\ \hat{e} &= P_A^\perp y \end{aligned} \tag{5}$$

In Eq. (5), N is a matrix with dimensions of $p \times p$, l is a vector with dimensions of $p \times 1$, $P_A^\perp$ is a orthogonal projection matrix, Q_i and Q_j in this study are cofactor matrices for code and phase observations, $\hat{e}$ is a residual vector, and $\hat{\sigma}$ is an unknown variance component. See (Amiri-Simkooei 2007) for more details on formulas.

Implementation of the LS-VCE method in PPP

Considering that in this research, the formation of a stochastic model and reaching the weight matrix has been done based on the LS-VCE method, the following is how to implement it in PPP positioning. In general, the structure of the stochastic model can be considered to consist of two parts. The first part includes the variance and accuracy of IF code and phase observations, and the second part presents a relation to express the dependence on the elevation angle of the satellite (Zangeneh-Nejad et al. 2018; Parvazi et al 2020; Qian et al. 2016). Hence, the covariance matrix for an epoch with n satellites will be made as follows:

$$\Sigma_C = \sigma_{P_{\text{IF}}}^2 Q_1 + \sigma_{\Phi_{\text{IF}}}^2 Q_2 \tag{6}$$

where $\sigma_{P_{\text{IF}}}^2$ and $\sigma_{\Phi_{\text{IF}}}^2$ are the variances of IF code and phase observations, respectively. At this step, we have two unknowns for each satellite system in each of the epoch with n satellites because the satellite's elevation-dependence is not considered. This signifies that now there exist four unknowns in the model by combining the Galileo and GPS systems. The dimensions of the co-factor matrices and their structure for observational epochs have been presented as follows:

$$(Q)_{2nk \times 2nk} = \Sigma_C \otimes \left(Q_E\right)_{nk \times nk} \tag{7}$$

In Eq. (7), Σ_C is a 2×2 matrix whose components (code and phase accuracy) are obtained by LS-VCE method. Q_E is the part of the stochastic model that represents the dependence of weight on the elevation angle of the satellite. In this study, due to the low sampling rate, the time correlation was considered absent. How to calculate this time correlation can also be followed in the study of Amiri-Simkooei et al. (2013), Bona (2000), and Li et al. (2008).

Recursive least-squares method and its implementation in PPP

In this study, in order to do the precise point positioning, we tend to implement the process epoch by epoch using RLS method. The RLS method was first proposed by Zangeneh-Nejad et al. in 2018 (Zangeneh-Nejad et al., 2018). If there is a non-linear relationship between observations and unknowns, this model can be presented as follows (Zangeneh-Nejad et al. 2018):

$$E\left\{\begin{pmatrix}\widehat{x}_1^{(1)}\\ y_2\end{pmatrix}\right\}=\begin{pmatrix}x_1\\ F_2(x_1,x_2)\end{pmatrix};D\left\{\begin{pmatrix}\widehat{x}_1^{(1)}\\ y_2\end{pmatrix}\right\}=\begin{pmatrix}Q_{\widehat{x}_1^{(1)}}0\\ 0\ Q_2\end{pmatrix}\tag{8}$$

where D and E are the observations dispersion and mathematical expectation operators respectively. F_1 and F_2 are the nonlinear vector functions from $R^{m_1}\to R^{n_1}$ and $R^{m_2}\to R^{n_2}$, respectively. $\widehat{x}_1^{(1)}$ is an estimate of x_1 and $Q_{\widehat{x}_1^{(1)}}$ covariance matrix of the first category of observations. By simplifying the equations as well as their linearization, the unknowns of both groups can be calculated as follows:

$$\begin{cases}\delta\widehat{x}_1^{(2)}=(^{Q_{\widehat{x}_1^{(1)}}^{-1}}[Q_{\widehat{x}_1^{(1)}}^{-1}(\widehat{x}_1^{(1)}-x_1^0)+\overline{A}_{21}^{0T}Q_2^{-1}(y_2-F_2(x_1^0,x_2^0))]\\ \delta\widehat{x}_2=(^{A_{22}^{0T}}[A_{22}^{0T}Q_2^{-1}(y_2-F_2(x_1^0,x_2^0))-A_{22}^{0T}Q_2^{-1}A_{21}^0\delta\widehat{x}_1^{(2)}]\end{cases}\tag{9}$$

where $\widehat{x}_1^{(1)}=\left(A_{11}^TQ_1^{-1}A_{11}\right)^{-1}A_{11}^TQ_1^{-1}y_1$, $Q_{\widehat{x}_1^{(1)}}=\left(A_{11}^TQ_1^{-1}A_{11}\right)^{-1}$, $A_{21}^0=\partial_{x_1}F_2\left(x_1^0,x_2^0\right)$ and $A_{22}^0=\partial_{x_2}F_2\left(x_1^0,x_2^0\right)$ are Jacobian matrices, and ∂_{x_1} represents the vector gradient relative to the vector. A_i design matrix, y_i observations vector, x_i unknown vector, and Q_i covariance variance matrix. Index i specifies the group of observations. x_1^0, x_2^0 the initial values are related to the taylor expansion. Then unknowns will be updated using the relations $\widehat{x}_1^{(2)}=x_1^0+\delta\widehat{x}_1^{(2)}$ and $\widehat{x}_2=x_2^0+\delta\widehat{x}_2$. The same process is repeated by replacing x_1^0 with $\widehat{x}_1^2$ and x_2^0 with $\widehat{x}_2$, and the iteration will continue until the convergence is achieved. The unknown vectors are defined as $x_1=\left(x_r,y_r,z_r,N_{IF}\right)$ and $x_2=\left(cdt_r,T_r\right)$. For more details on the equations presented and their proofs, please refer to Zangeneh-Nejad et al. (2018).

The procedure for horizontal deformation analysis

The deformation analysis is, in fact, a method of determining the displacement of fixed points, as well as significant displacements in geodetic networks (Amiri-Simkooei et al. 2017, 2012; Kalkan et al. 2016). The false assumptions about the assumed fixed points in a geodetic network can have serious consequences in interpreting the displacements of points or predicting the displacement of structures. Therefore, one of

the important steps in deformation analysis is to determine the meaning of the displacement that occurred at the points, which is done using statistical tests. It is noteworthy that the displacement evaluation is typically performed in local coordinate systems; in this study, the results and the equations required to achieve the displacement vector based on the ENU coordinate system are presented (Vodopivec and Savsek-Safic 2003; Savšek-Safić et al. 2006). The deformation created at a point can be defined as the statistical significant displacement of that point in two different epochs. For example, the position of a point at time t is expressed as $P_t\left(\text{East}_t,\text{North}_t\right)$ using the covariance matrix ΣP_t and at time $t+dt$ as $P_{t+dt}\left(\text{East}_{t+dt},\text{North}_{t+dt}\right)$ using the covariance ΣP_{t+dt}. The amount of displacement, horizontal displacement, and covariance matrix related to the point coordinates is defined by the difference between the estimated coordinates at times t and $t+dt$ as follows (Koch 1999; Vodopivec and Savsek-Safic 2003; Savšek-Safić et al. 2006; Alcay et al. 2019):

$$\begin{cases}P_{t+dt}-P_t=\begin{bmatrix}East_{t+dt}-East_t\\ North_{t+dt}-North_t\end{bmatrix}==\begin{bmatrix}\Delta East\\ \Delta North\end{bmatrix}\\ d=\sqrt{\Delta East^2+\Delta North^2}\\ \Sigma P_t=\begin{bmatrix}\sigma_{East_t}^2 & \sigma_{East_t,North_t}\\ \sigma_{North_t,East_t} & \sigma_{North_t}^2\end{bmatrix}\\ \Sigma P_{t+dt}=\begin{bmatrix}\sigma_{East_{t+dt}}^2 & \sigma_{East_{t+dt},North_{t+dt}}\\ \sigma_{North_{t+dt},East_{t+dt}} & \sigma_{North_{t+dt}}^2\end{bmatrix}\\ Azimuth\_angle=\text{atan}(\frac{\Delta East}{\Delta North})\end{cases}\tag{10}$$

Assuming the coordinates in the two epochs t and $t+dt$ are uncorrelated, the covariance matrix for the coordinates of point in two epochs can be expressed as follows (Vodopivec and Savsek-Safic 2003; Savšek-Safić et al 2006):

$$\Sigma P_t P_{t+dt}=\begin{bmatrix}\sigma_{East_t}^2 & \sigma_{East_t,North_t} & 0 & 0\\ \sigma_{North_t,East_t} & \sigma_{North_t}^2 & 0 & 0\\ 0 & 0 & \sigma_{East_{t+dt}}^2 & \sigma_{East_{t+dt},North_{t+dt}}\\ 0 & 0 & \sigma_{North_{t+dt},East_{t+dt}} & \sigma_{North_{t+dt}}^2\end{bmatrix}\tag{11}$$

The variance of horizontal displacement by considering the Jacobi matrix J_d can be written as follows (finally, by calculating the multiplication of these matrices, the standard deviation(STD) of displacement (σ_d) is presented) (Vodopivec and Savsek-Safic 2003; Savšek-Safić et al 2006)::

$$\begin{cases}\sigma_d^2=J_d\Sigma P_t P_{t+dt}J_d^T\\ J_d=\begin{bmatrix}\frac{\partial d}{\partial East_t} & \frac{\partial d}{\partial North_t} & \frac{\partial d}{\partial East_{t+dt}} & \frac{\partial d}{\partial North_{t+dt}}\end{bmatrix}=\begin{bmatrix}-\frac{\Delta East}{d} & -\frac{\Delta North}{d} & \frac{\Delta East}{d} & \frac{\Delta North}{d}\end{bmatrix}\\ \sigma_d=\sqrt{(\frac{\Delta East}{d})^2(\sigma_{East_t}^2+\sigma_{East_{t+dt}}^2)+(\frac{\Delta North}{d})^2(\sigma_{North_t}^2+\sigma_{North_{t+dt}}^2)+2\frac{\Delta East}{d}\frac{\Delta North}{d}(\sigma_{East_t,North_t}+\sigma_{East_{t+dt}North_{t+dt}})}\end{cases}\tag{12}$$

In this study, the deformation calculation has been performed continuously, signifying that the data of the first epoch is used as a reference and that the second epoch is compared with the reference epoch.

Statistical tests of displacement significance

In regard to calculating displacement, we presented the results based on a comparison between two epochs. In the following, we considered two hypotheses, namely the null hypothesis and alternative hypothesis as follows (Koch 1999; Savšek-Safić et al. 2006; Alcay et al. 2019):

$$\begin{cases} H_0 : E(d) = 0 & \textit{No displacement between two epochs} \\ H_0 : E(d) \neq 0 & \textit{Displacement between two epochs} \end{cases}$$
(13)

After the adjustment of at least two time epochs, we can determine the displacement d based on the second term of Eq. (10) and the displacement standard deviation σ_d using the third term of Eq. (12). Since these two parameters can be calculated before deformation analysis, they are used properly in statistical tests so that we can consider the test statistics as follows (Savšek-Safić et al 2006):

$$T_{\text{test}} = \frac{d}{\sigma_d}$$
(14)

At last, the value of T_{test} for each point is compared with the critical value T_{crit} at a confidence level α. To know whether the displacement is significant or not, if $T < T_{\text{crit}}$, the null hypothesis will be confirmed and therefore the displacement will not be statistically valid. If $T > T_{\text{crit}}$, the null hypothesis will be rejected and the displacement will be statistically valid; for more details about the critical value (T_{crit}), that is, its method of calculation, formulation, and determination, see Savšek-Safić et al. (2006). As described in Savšek-Safić et al. (2006), the value of T_{crit} is equal to 3. As a "rule of thumb," its value is larger than that obtained from the distribution function of the test statistics. Therefore, in this research, "3" is considered as the critical value.

Experimental tests, processing strategy, and results

The combination of multi-GNSS observations for Galileo and GPS includes E1/E5a and L1/L2 signals, respectively. Therefore, estimation of model unknowns is done by observations of these two systems. Table 1 shows the observation processing strategy for the combined multi-GNSS precise point positioning. The observations used in this part of the study were collected by the a multi-GNSS receiver on April 24, 2018, in two epochs. A high-precision device was used to simulate the point displacement at the horizontal level. Figure 2 shows the device used along with the displacement value. In this study, a horizontal displacement test was

Table 1 Information used along with settings made in PPP processing

Item	Setting
Observables	Undifferenced code and phase observations
Frequency	Galileo: E1/E5a; GPS: L1/L2
Elevation Cutoff	$10°$
process	Positioning using a combination of multi-GNSS (Galileo and GPS) observations
Estimator	RLS with the unknowns added (Zangeneh-Nejad et al. 2018)
Stochastic model	Nominal weight (code = 2 m and phase 15 mm) $\sigma_{G,P} : \sigma_{E,P} = 1 : 2, \sigma_{G,L} : \sigma_{E,L} = 1 : 2$
Sampling rate	5^s
Satellite orbit and clock	GFZ multi-GNSS
Satellite antenna PCO and PCV	GPS, Galileo: IGS14.atx
Receiver antenna phase center and variation	IGS14.atx
Troposphere model	Saastamoinen model and global mapping function (GMF) (Böhm et al., 2006)
Relativistic correction	Corrected (Prokopov et al., 2009)
Phase wind-up	Corrected (Wu et al., 1992)
Station displacement	Ocean tide loading, solid earth tides, and pole tides (Kouba and Héroux 2001)
Observation weight	By LS-VCE method
Processing mode	Static
Adjustment method	PPP solution: RLS algorithme (Zangeneh-Nejad et al. 2018)
Estimated parameters	System time difference parameters, receiver clock error, receiver position, ambiguity parameters, and tropospheric wet delay
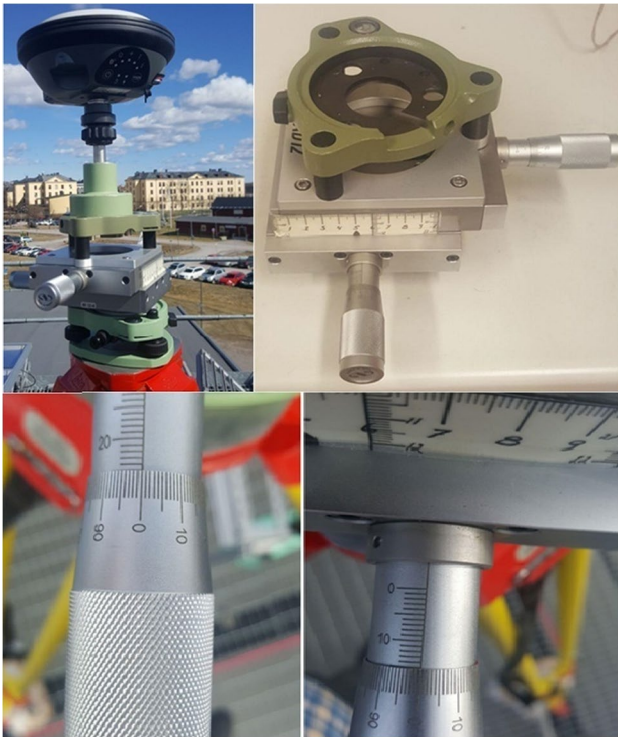
Fig. 2 The device used to apply the simulated displacement with the receiver (15 mm on the right side of displacement, 25 mm on the left side of displacement for the north and east components)

performed, involving the application of displacements (15 and 25 mm) for the north and east horizontal components. The amount of simulated displacement between the two epochs has been considered as a real displacement.

In this research, observations in two epochs have been used. Initially, processing was performed as PPP using the five weight models presented. Observations were analyzed by nominal stochastic model and estimated model by LS-VCE method. In the nominal method, the observation accuracy of code 2 m and phase 15 mm was selected. In the second method, the stochastic model was estimated according to LS-VCE. Figures 3 and 4 show the standard deviations of the GPS code and phase observations with the five models. Also in Figs. 5 and 6, the results of the Galileo system are presented. Table 2 shows the mean values of the standard deviations for the GPS code and phase. According to this table, the values estimated by the LS-VCE method are different from their nominal values.

Deformation analysis using GPS-only measurements

In this section, by using GPS observations and considering different weighting models, the displacement analysis has been studied. The results have been reviewed in several ways. Initially, the volume of displacement in the direction of the two components of east and north will be presented in

Fig. 3 The STD of code and phase (GPS) parameters using LS-VCE in the first Epoch (duration of observations: 3 h and 50 min): code (above the picture) and phase (below the picture)
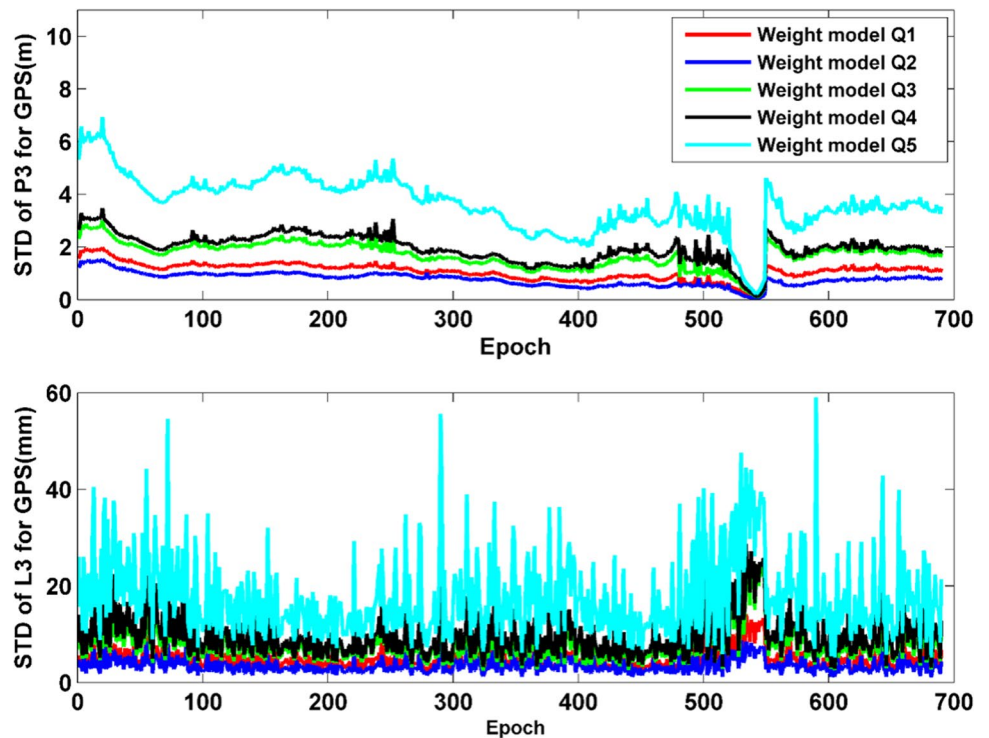
Fig. 4 The STD of code and phase (GPS) parameters using LS-VCE in the second Epoch (duration of observations: 4 h and 12 min): code (above the picture) and phase (below the picture)
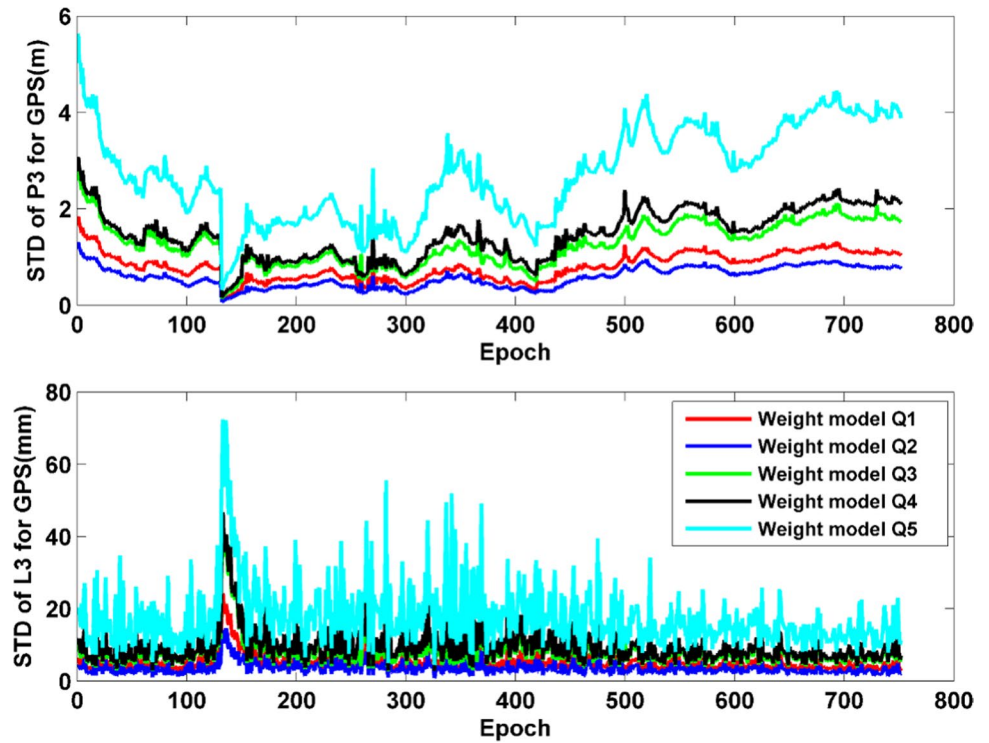
Fig. 5 The STD of code and phase (Galileo) parameters using LS-VCE in the first Epoch (duration of observations: 3 h and 50 min): code (above the picture) and phase (below the picture)
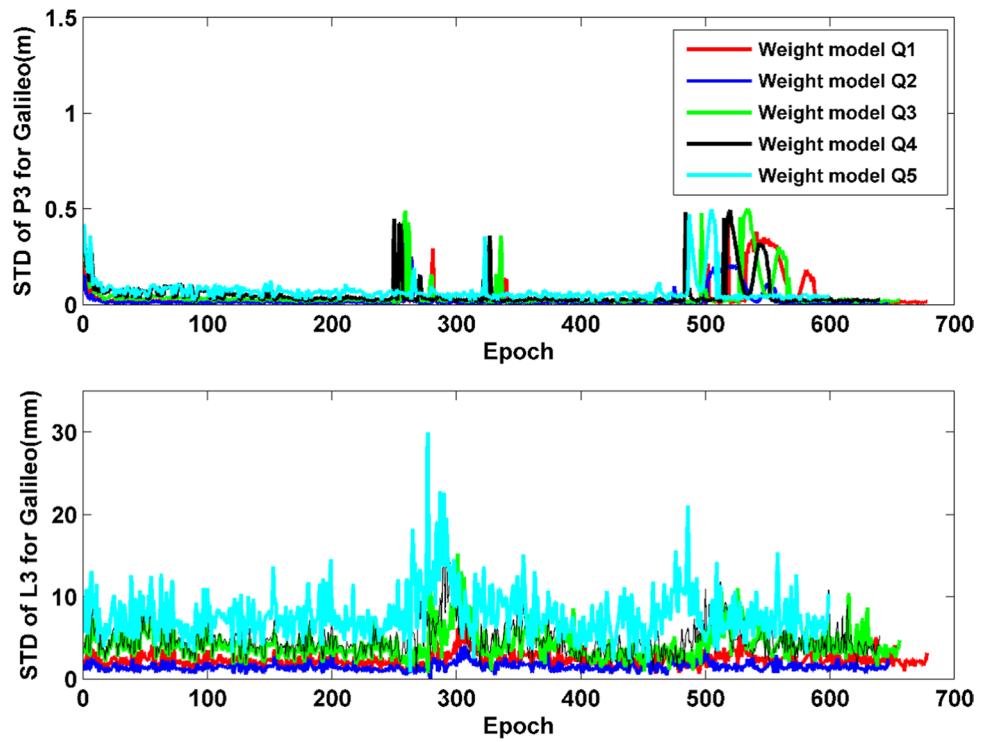
two epochs. Then the standard deviation related to these two components will be tested. Following that, the two-dimensional displacement vectors and azimuths will be analyzed. At last, by performing the statistical tests, the significance of the displacement will be examined. The results have been evaluated in the two modes of using the nominal weight and the estimated weight. In order to evaluate the performance of the proposed method, Table 3 has presented the results of the displacement for the desired point in two epochs using the nominal stochastic model and estimated stochastic model

Fig. 6 The STD of code and phase (Galileo) parameters using LS-VCE in the second Epoch (duration of observations: 4 h and 12 min): code (above the picture) and phase (below the picture)
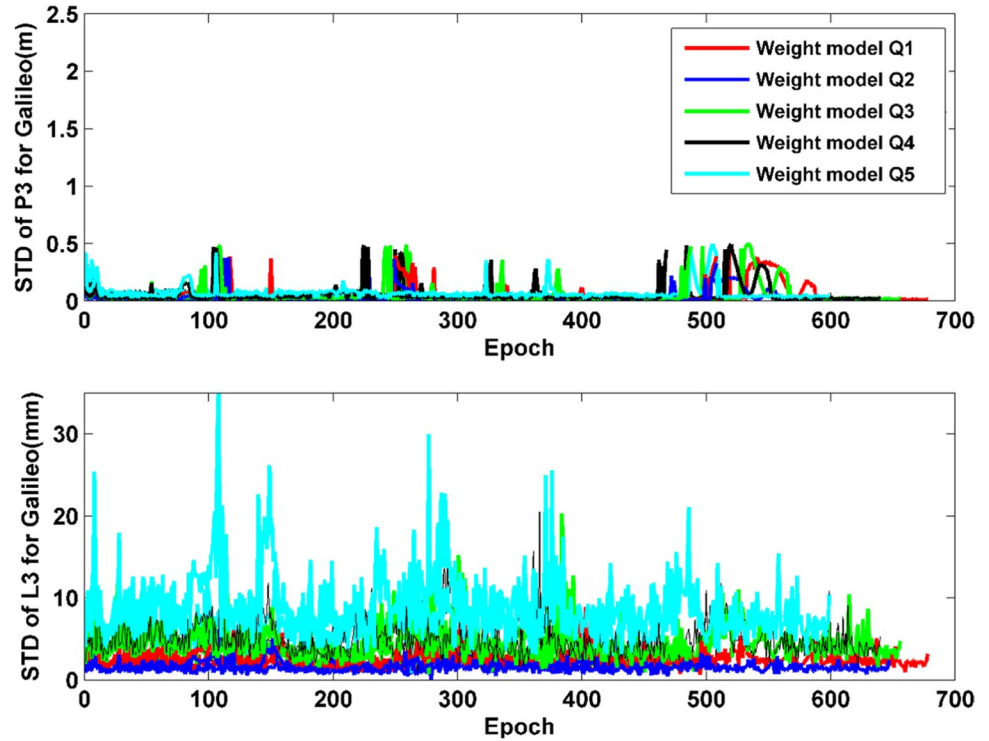
Table 2 The mean STD of code and phase (GPS/Galileo) parameters

Component	Weight (Q_1)	Weight (Q_2)	Weight (Q_3)	Weight (Q_4)	Weight (Q_5)
$\sigma_{P3}^{GPS}(m)$ – Epoch_1	1.072	0.776	1.703	1.956	3.626
$\sigma_{L3}^{GPS}(mm)$ – Epoch_1	4.8	3.5	8.3	9.8	17.4
$\sigma_{P3}^{GPS}(m)$ – Epoch_2	0.800	0.574	1.279	1.468	2.717
$\sigma_{L3}^{GPS}(mm)$ – Epoch_2	6.6	4.3	11.8	13.1	22.2
$\sigma_{P3}^{Galileo}(m)$ – Epoch_1	0.06	0.08	0.08	0.11	0.35
$\sigma_{L3}^{Galileo}(mm)$ – Epoch_1	2.4	1.6	4.3	4.8	7.9
$\sigma_{P3}^{Galileo}(m)$ – Epoch_2	0.23	0.17	0.45	0.59	0.86
$\sigma_{L3}^{Galileo}(mm)$ – Epoch_2	2.5	1.7	4.4	4.9	8.5

Table 3 Compare the results obtained for the displacement of the east–west and north–south components using two nominal stochastic models and LS-VCE in the precise point positioning method with the help of GPS observations at the two time intervals of 4 h

Weight matrix	Estimated value with nominal weighting model			Estimated value with LS-VCE weighting model			Actual displacement	
	East (mm)	North (mm)	Difference	East (mm)	North (mm)	Difference	East (mm)	North (mm)
Q1	19.7	− 23.0	− 5.3 − 8	21	− 20.7	− 4 − 5.7	25	− 15
Q2	20.8	− 15.9	− 4.2 − 0.9	18.6	− 12	− 6.4 − 3	25	− 15
Q3	22.4	− 26.4	− 2.6 − 11.4	26.6	− 23.9	1.6 − 8.9	25	− 15
Q4	22.3	− 21.6	− 2.7 − 6.6	27.5	− 19.5	2.5 − 4.5	25	− 15
Q5	23.1	− 16.1	− 1.9 − 1.1	25	− 13.1	0 1.9	25	− 15

by LS-VCE method. The first epoch is considered as a reference epoch.

According to the results presented in Table 3, by using 5 nominal weight models for stochastic model to estimate the east–west and north–south components, the weighting model Q_5 becomes more accurate in estimating these components. Thus, as compared with the real displacement, the difference for the East–West component is − 1.9 mm and for

the North–South component is − 1.1 mm. In the same case, when the LS-VCE method is used for the precision estimation of IF code and phase parameters instead of the nominal weight, the weighting model Q_5 becomes more accurate in estimating the east–west and north–south components, also for the east–west component, there is no difference between the estimated value and the real value, and for the north–south component the difference is − 1.9 mm. Based on these results, for the components weight estimation of the IF code and phase, the LS-VCE method is more accurate and this increase in efficiency has been presented in the four used models. In Table 4, the estimated standard deviation parameter has been presented by the LS-VCE method for each of the two East–West and North–South components by using the nominal and estimated weights.

According to the obtained results, in all different weighting modes, using the LS-VCE method is more accurate than utilizing the nominal weight in presenting the east–west and north–south components. Based on the results of Table 4, in the first epoch, for the East–West component, the highest precision is 0.9 mm when using the weighted model Q_5 and the lowest precision is 5.9 mm when using the weighted model Q_2; for the North–South component, the highest precision is 0.5 mm when using weighted model Q_5, and the lowest precision is 3.8 mm when using the weighted model Q_2. In the second epoch, the highest and lowest precisions

for the east–west component are 1.5 and 8.3 mm, respectively and for the north–south component they are 0.7 and 4.2 mm, respectively.

To compare the results when using the LS-VCE method in the weight estimation of the IF code and phase in the first and second epoch, regardless of which weighting model is used, the highest and lowest precisions for the east–west component are 0.3 to 0.5 mm and for the north–south component the precision is 0.2 mm. Based on these results, the precision improvement when using the LS-VCE method for the East–West component is between 0.6 and 7.8 mm and for the North–South component it is between 0.3 and 4 mm, which indicates a significant increase in precision when using the LS-VCE method. Table 5 presents the results of the displacement vector and its relevant azimuth.

According to Table 5, which is, in fact, a supplement to the information obtained from Table 3, it can be seen that when using the weight model Q_5 and Q_1, the precise point positioning method using the weight estimation with LS-VCE compared to the nominal weight can cause us to approach the exact value of displacement, that is, the real displacement. In fact, first of all, the main criterion is that the estimated values must be close to the real value in two east–west and north–south directions. Secondly, the displacement vector needs to be close to the real value. On

Table 4 Comparison of the results obtained for the precision of East–West and North–South components using the two models of nominal stochastic and LS-VCE in the precise point positioning method by GPS observations at two time intervals of 4 h

Weight matrix	STD. with nominal weighting model				STD. with LS-VCE weighting model			
	Epoch.1		Epoch.2		Epoch.1		Epoch.2	
	East (mm)	North (mm)	East (mm)	North (mm)	East (mm)	North (mm)	East (mm)	North (mm)
Q1	3.1	1.8	5.1	2.4	0.3	0.2	0.5	0.2
Q2	5.9	3.8	8.3	4.2	0.3	0.2	0.4	0.2
Q3	1.9	1.1	3.1	1.5	0.3	0.2	0.5	0.2
Q4	1.7	1.0	2.7	1.3	0.3	0.2	0.5	0.2
Q5	0.9	0.5	1.5	0.7	0.3	0.2	0.5	0.2

Table 5 Estimated displacement and azimuth using the two models of stochastic nominal and LS-VCE in the PPP method by GPS observations at two time intervals of 4 h

Weight matrix	Estimated value with nominal weighting model				Estimated displacement with LS-VCE weighting model				Actual	
	d (mm)	Azimuth (°)	Difference		d (mm)	Azimuth (°)	Difference		d (mm)	Azimuth (°)
			d	Az			d	Az		
Q1	30.28	− 40.58	1.13	18.46	29.49	− 45.41	0.34	13.63	29.15	− 59.04
Q2	26.18	− 52.60	− 2.97	6.44	22.14	− 57.17	− 7.01	1.87	29.15	− 59.04
Q3	34.62	− 40.31	5.47	18.73	35.76	− 48.06	6.61	10.98	29.15	− 59.04
Q4	31.05	− 45.91	1.90	13.13	33.71	− 54.65	4.56	4.39	29.15	− 59.04
Q5	28.16	− 55.12	− 0.99	3.92	28.22	− 62.34	− 0.93	− 3.30	29.15	− 59.04

Table 6 Statistical tests in displacement detection

Weight matrix	Nominal weighting model				LS-VCE weighting model			
	σ_d(mm)	T_{test}	T_{crit}	Displacement	σ_d(mm)	T_{test}	T_{crit}	Displacement
Q1	4.26	7.1	3	Yes	0.39	73.9	3	Yes
Q2	8.9	2.9	3	No	0.44	49.9	3	Yes
Q3	2.63	13.2	3	Yes	0.43	83.0	3	Yes
Q4	2.48	12.5	3	Yes	0.47	72.3	3	Yes
Q5	1.48	18.9	3	Yes	0.47	58.9	3	Yes

the other hand, detecting the azimuth angle in the precise point positioning with the help of the estimated weight using the LS-VCE method is more accurate than using the nominal weight. After obtaining the displacement value in the two directions of the east–west and north–south, the results related to the displacement vector precision, as well as doing statistical tests must be performed to examine the significance of the displacement. The relevant results have been presented in Table 6.

The results presented in Table 6 are interpreted in two manners. At first, a comparison is made between the standard deviation obtained for the displacement component *d* in the two cases of using the nominal weight and estimated weight with the help of LS-VCE in the precise point positioning method in such a manner that when the nominal weight is used, in this case the highest precision of the precise point positioning method is 1.48 mm when using the weighting model Q_5 and the lowest precision is 8.9 mm in the weighting model Q_2. In case of using the estimated weight with the help of LS-VCE, the same examination

shows a value between 0.4 and 0.5 mm. Therefore, by comparing the results of Table 6, it can be shown that the precise point positioning when using the estimated weight with the help of LS-VCE can improve the precision of the displacement component between 1 and 9 mm.

Given the effect that different stochastic models can have on the quality of the position obtained from GNSS observations (Hadas et al. 2020; Li et al. 2016; Luo et al. 2014), to further evaluate the better stochastic model, it is possible to provide a more accurate evaluation for the coordinates of the points. Therefore, for the desired station, considering the relevant stochastic models in two epochs, the results related to the standard deviation of the coordinates have been evaluated. Figures 7, 8, 9, and 10 show the standard deviation of the east–west and north–south components. Also, Fig. 11 shows the estimated mean precision for two-dimensional coordinate components using five stochastic models.

According to Figs. 7 to 11, it can be observed that in the first and second epochs, when different stochastic models
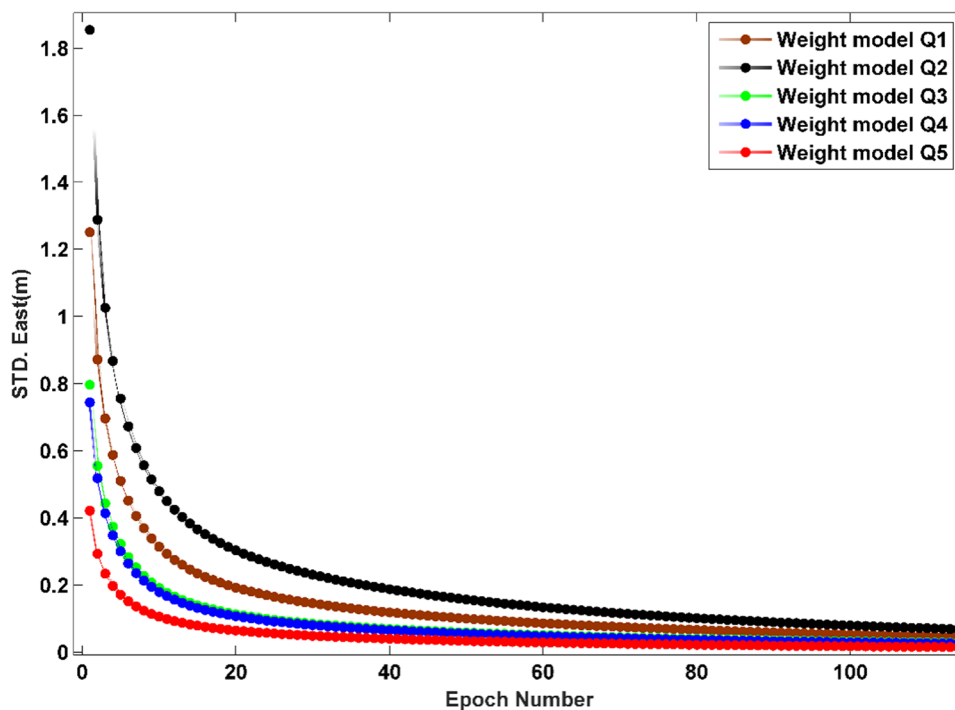

Fig. 7 East–West component standard deviation using five stochastic models in the first epoch
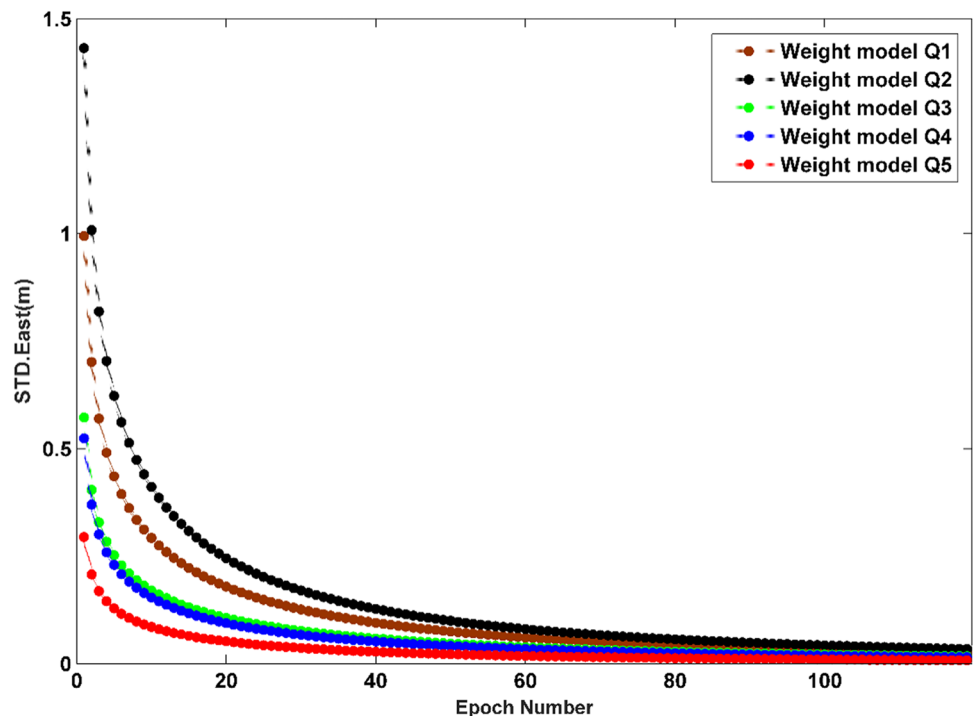
Fig. 8 North–South component standard deviation using five stochastic models in the first epoch
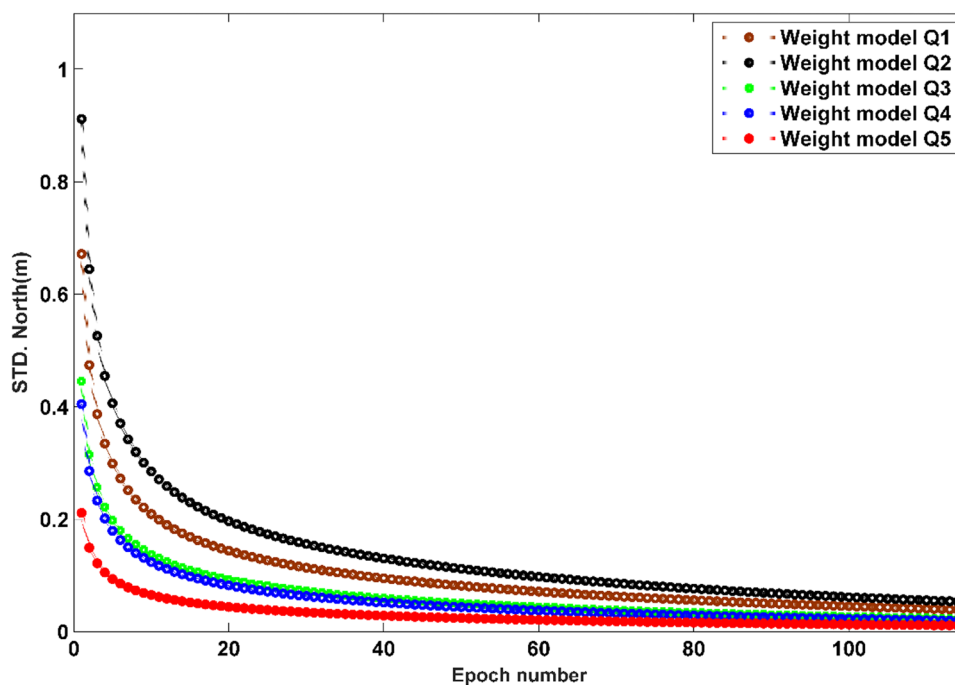
Fig. 9 East–West component standard deviation using five stochastic models in the second epoch


are utilized, the exponential stochastic model and cosine stochastic model offer better precision for coordinate components so that the use of the exponential stochastic model can have the highest accuracy. The precision of the estimated coordinates is one of the criteria that can be used for the superiority of these models. At last, for the best model (the exponential model), the maximum value of the standard deviation in the two epochs for the east–west and north–south components is between 21 and 42 cm and the minimum value is between 0.1 and 0.3 mm.

Deformation analysis using multi-GNSS (Galileo and GPS) measurements

In this section, the displacement analysis with the combination of systems has been discussed. In order to investigate

Fig. 10 North–South component standard deviation using five stochastic models in the second epoch
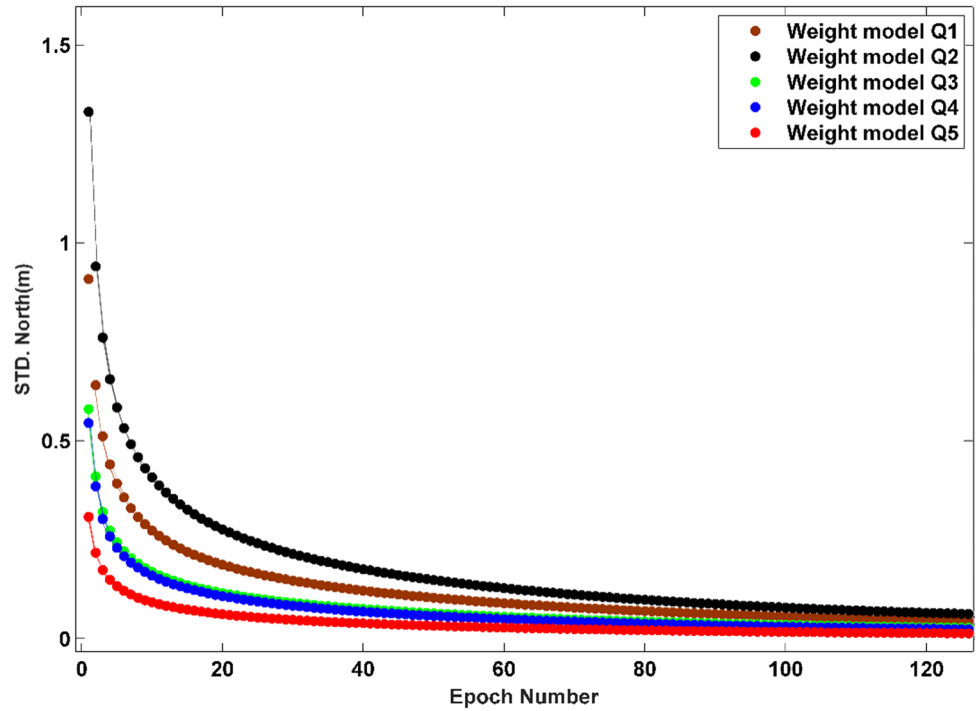
Fig. 11 Estimated mean precision for two-dimensional coordinate components using five stochastic models
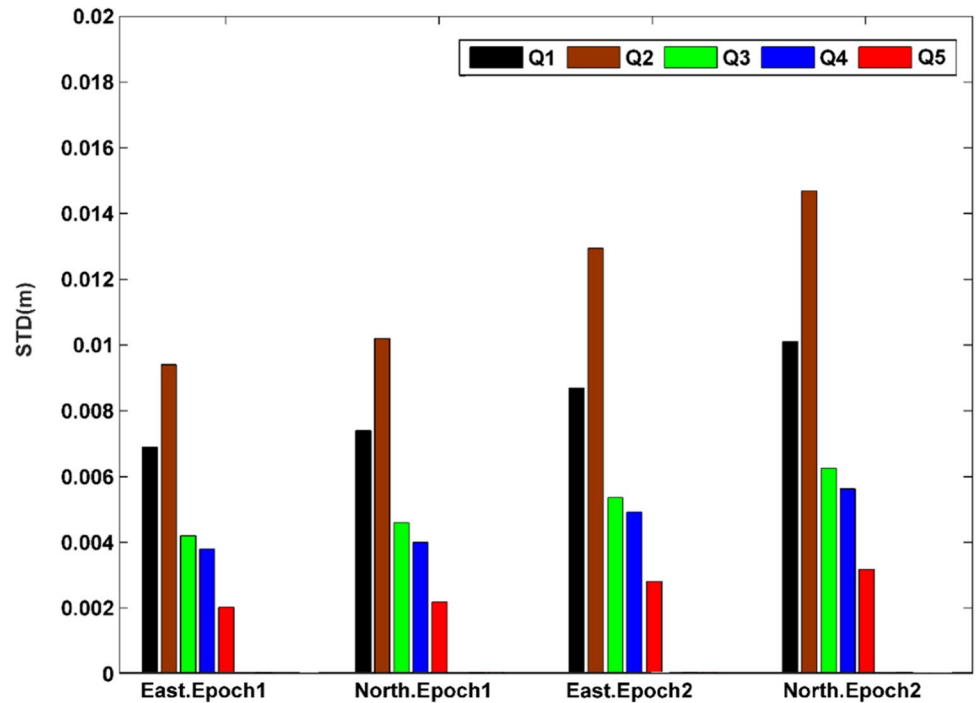
the combination of different satellite systems observations, we used the multi-GNSS observations. According to the mode of using satellite single-system observations, in this section we have examined all the features mentioned above when multi-GNSS observations are combined. Initially, the displacement comparison of the east–west and north–south components was made using the two nominal stochastic

models and the LS-VCE method in the precise point positioning method with the help of the multi-GNSS observations. The results of this comparison have been presented in Table 7.

Based on the results presented in Table 7, it can be seen that when a combination of multi-GNSS observations is used, the numerical values of the components estimated

in case of using the nominal weight and the estimated weight are close to each other. The weight estimation has a greater effect on the coordinate estimation than nominal weight when only GPS is used. With respect to the combined observations, the use of the Q5 weight model can provide the estimated coordinates at the values which are the closest to the actual coordinates. Then the precision of the components of the east–west and north–south components was compared using two weighting models in the PPP method. The results of this comparison have been presented in Table 8.

According to Table 8, it can be seen that in case of combination of multi-GNSS observations when the precision estimation is utilized for code and phase components, the

estimated precision for North–South and East–West coordinate components with LS-VCE method has been improved by 5.8 mm compared to the nominal weight. This increase in precision is 0.7 mm for the combined mode compared to GPS-only. Afterward, the displacement analysis and the estimated azimuth have been discussed using the two models. The results of this comparison have been presented in Table 9.

Based on the results presented in Table 9, in most cases the estimated two-dimensional displacement in the case of the estimated weight relative to the nominal weight presents a result closer to reality. The LS-VCE method presupposes a realistic weight matrix estimated from your data. Therefore, another criterion that can be chosen for comparison is the

Table 7 Comparison of displacement of east–west and north–south using the two models of nominal stochastic and LS-VCE in the PPP method with the multi-GNSS observations

Weight matrix	Estimated value with nominal weighting model				Estimated value with LS-VCE weighting model				Actual displacement	
	East (mm)	North (mm)	Difference		East (mm)	North (mm)	Difference		East (mm)	North (mm)
Q1	21.8	−24.9	−3.2	−9.9	21.3	−24.9	−3.7	−9.9	25	−15
Q2	18.5	−18.3	−6.5	−3.3	18.1	−18.4	−6.9	−3.4	25	−15
Q3	24.3	−27.8	−0.7	−12.8	24.0	−27.6	−1	−12.6	25	−15
Q4	21.5	−23.2	−3.5	−8.2	21.1	−23.1	−3.9	−8.1	25	−15
Q5	20.2	−18.2	−4.8	−3.2	19.7	−18.2	−5.3	−3.2	25	−15

Table 8 Comparison of the precision of east–west and North–South components using the two models of nominal stochastic and LS-VCE in the PPP method with the multi-GNSS observations

Weight matrix	STD. with nominal weighting model				STD. with LS-VCE weighting model			
	Epoch.1		Epoch.2		Epoch.1		Epoch.2	
	East (mm)	North (mm)	East (mm)	North (mm)	East (mm)	North (mm)	East (mm)	North (mm)
Q1	1.7	2.9	2.3	4.6	0.3	0.2	0.6	0.3
Q2	2.4	4.0	3.0	6.4	0.3	0.2	0.6	0.3
Q3	1.1	1.8	2.8	2.8	0.3	0.2	0.6	0.3
Q4	0.9	1.6	1.3	2.4	0.3	0.2	0.6	0.3
Q5	0.5	0.8	0.7	1.3	0.3	0.2	0.6	0.3

Table 9 Estimated displacement and azimuth using the two models of nominal stochastic and LS-VCE in the PPP method with the multi-GNSS observations

Weight matrix	Estimated value with nominal weighting model				Estimated displacement with LS-VCE weighting model				Actual	
	d (mm)	Azimuth (deg)	Difference		d (mm)	Azimuth (deg)	Difference		d (mm)	Azimuth (deg)
			d	Az			d	Az		
Q1	33.07	−41.20	3.92	17.84	32.77	−40.54	3.62	18.50	29.15	−59.04
Q2	26.04	−45.31	−3.11	13.73	25.75	−44.53	−3.40	14.51	29.15	−59.04
Q3	36.91	−41.16	7.76	17.88	36.62	−41.01	7.47	18.03	29.15	−59.04
Q4	31.63	−42.82	2.48	16.22	31.23	−42.41	2.08	16.63	29.15	−59.04
Q5	27.21	−47.98	−1.94	11.06	26.79	−47.27	−2.36	11.77	29.15	−59.04

Table 10 The results related to statistical tests to examine the significance of displacement using the two models of nominal stochastic and LS-VCE in the PPP method with the multi-GNSS observations

Weight matrix	Nominal weighting model				LS-VCE weighting model			
	σ_d(mm)	T_{test}	T_{crit}	Displacement	σ_d(mm)	T_{test}	T_{crit}	Displacement
Q1	4.0	8.3	3	Yes	0.5	66.5	3	Yes
Q2	5.8	4.5	3	Yes	0.5	51.3	3	Yes
Q3	2.4	15.1	3	Yes	0.5	68.8	3	Yes
Q4	2.2	14.4	3	Yes	0.6	56.8	3	Yes
Q5	1.3	21.3	3	Yes	0.6	48.2	3	Yes

estimated precision for the displacement, which is calculated in two ways. At last, the results related to the statistical tests and the significance of the estimated displacement have been evaluated. The results of this comparison have been presented in Table 10.

An increase in precision for the displacement component is 5.3 mm when the estimated weight is used compared to the nominal weight. In all different weighting modes, the combination of observations has increased the estimated precision of the displacement component compared to the single-system mode. In case of the combination of multi-GNSS observations, in all different weighting modes, the displacement significance test even when the nominal weight is used has been confirmed. When the observations are combined, in most cases the difference between the estimated coordinate components with the real value of displacement has decreased. Sometimes, the combination of systems is not able to present less difference for displacement than the single-system mode, resulting from the low number of satellites tracked by the Galileo positioning system.

The capability of the PPP method in detecting stable points

To evaluate the PPP method in the displacement analysis more accurately, instead of estimating the numerical value of the displacement in both east and north directions, this analysis is conducted to determine whether the studied station has been displaced or not. A four-point was used for this study. The observations were made for each station at two intervals of 5 h. Stations 1 and 2 were fixed throughout the measurement period, and the stations 3 and 4 were moved in the second epoch. In view of the fact that the receivers are fixed on the concrete pillar of the station, it is not possible to change them unless this change of motion is intentionally applied to the points. For stations 3 and 4, this displacement was applied using a special device installed on the pillar. When the receivers moved from their initial location at stations 3 and 4, the other three receivers at points 1 and 2 remained unchanged at their initial location without any interruption in the observation. The observations for the four stations in the two time epochs have been presented in Table 11.

To evaluate the results, two observation periods were performed on the desired stations. As mentioned earlier, for the stations 3 and 4, the two receivers were moved to their initial positions. Yet the other three stations were continuously taking the observations in the two epochs without relocation. Table 12 shows the position of four stations with their standard deviations in the UTM coordinate system. Also, Table 13 reveals the amount of two-dimensional displacement of points, as well as the estimated displacement.

This section replies to the questions as to whether the approach is to detect the magnitude of the displacement at points, and whether only the PPP method is used to move the points, and whether this method is capable of correct diagnosis or not. According to the results presented in Tables 12 and 13, it can be observed that sometimes the estimated amount of displacement differs from the actual displacement. Yet this method can also be used to confirm

Table 11 Time of collecting observations at each station

Station Number		Epoch_1			Epoch_2		
		Date	Time	Duration (h)	Date	Time	Duration (h)
1	Start	23.05.2018	9:50:0	5.66	23.05.2018	15:56:0	5.66
	End		15:30:0			21:36:0	
2	Start	23.05.2018	9:50:0	5.66	23.05.2018	15:56:0	5.66
	End		15:30:0			21:36:0	
3	Start	23.05.2018	9:50:0	5.66	23.05.2018	15:56:0	5.66
	End		15:30:0			21:36:0	
4	Start	23.05.2018	10:21:0	5.15	23.05.2018	15:56:0	5.15
	End		15:30:0			21:05:0	

Table 12 Coordinates and standard deviation of four stations in the UTM coordinate system

Station Number	Epoch_1				Epoch_2			
	UTM coordinate system							
	East (m)	STD (mm)	North (m)	STD (mm)	East (m)	STD (mm)	North (m)	STD (mm)
1	606,673.360	1.62	6,719,513.701	0.98	606,673.356	2.84	6,719,513.695	1.27
2	606,602.995	1.62	6,720,345.992	0.98	606,602.994	5.31	6,720,345.985	2.02
3	607,093.994	1.22	6,719,091.812	0.72	607,093.982	2.09	6,719,091.790	0.95
4	607,036.813	1.39	6,720,141.985	0.77	607,036.794	2.33	6,720,141.981	1.00

Table 13 Point displacement (Local ENU coordinate) analysis in the second case

Station Number	d estimated (mm)	d actual (mm)	T_{test}	T_{crit}	Displacement
1	6.7	0	2.76	3	No
2	6.6	0	2.88	3	No
3	24.5	17	14.52	3	Yes
4	18.9	9	7.01	3	Yes

whether the point has been displaced and whether this displacement is significant. Therefore, this method can also be used whether only one point is moved or not, which can be used for various applications that require a centimeter precision.

Conclusion

In this research, we studied the effect of the stochastic model in determining displacement. Three types of elevation-dependent stochastic model with five samples were used. The trigonometric *sinE* (two samples), trigonometric *cosE* (two samples), and exponential functions of one sample were employed. The RLS method was used to solve the PPP problem and the LS-VCE method was employed to determine the variance of GNSS observations. Evaluations and results show that the Q_5 model performed better analysis than other models. Therefore, the analysis of the results using this model was performed in several stages. The first step is to compare the differences between the actual and estimated coordinates for the east–west and north–south components using the nominal weight and the LS-VCE method. The results of the coordinate comparison show that the stochastic model based on the LS-VCE in the PPP method gives a difference of 0 and − 1.9 mm for the east–west and north–south components, while the use of nominal weight, a difference of − 1.9 and − 1.1 mm. In the second step, two weighting methods were studied in terms of estimating coordinate accuracy. The accuracy parameter for these components in two epochs, for the nominal weight mode, were between

0.9 to 8.3 mm (epoch1) and 0.5 to 4.2 mm (epoch 2) for five elevation-dependent model (Q_1–Q_5); meanwhile, in the case of using the LS-VCE method, these values were between 0.3 to 0.5 mm and 0.1 to 0.2 mm. Based on these results, should the LS-VCE be employed, the precision improvement for the East–West component will be between 0.6 and 7.8 mm, and for the North–South component will be between 0.3 and 4 mm. In the third step, after obtaining the coordinates, the accuracy parameter of the horizontal component was evaluated. Accordingly, the nominal weight mode provided an accuracy of this component between 1.48 and 8.9 mm, while the use of LS-VCE reduced this value to 0.4 to 0.5 mm. In the fourth step, instead of using GPS-only observations, Multi-GNSS observations were used for displacement analysis. Based on this, the estimated precision for the north–south and east–west coordinate components was increased by 5.8 mm when the LS-VCE was utilized compared to the nominal weight. The precision of the displacement component was increased by 5.3 mm by using the estimated weight compared to the nominal weight. Therefore, based on what was presented, it can be concluded that:

There are two factors influencing displacement analysis. One is the variance of the code and phase observations and the other is the elevation-dependent weight model.

The use of the LS-VCE method has yielded more favorable results in terms of both coordinates and their accuracy than the nominal weight mode. This accuracy improvement was also presented for the horizontal component.

The accuracy of the coordinates presented in the nominal weight mode is strongly influenced by the elevation-dependent weight model, while the LS-VCE method has fewer changes in the accuracy of the presentation by changing these models.

In both modes use only GPS and Multi-GNSS, the PPP method can provide us with more accurate displacement by using the LS-VCE weight estimation than the nominal weight.

Multi-GNSS mode has provided better results in estimating accuracy.

Therefore, the PPP method can also be used to verify whether the point is displaced and whether this displacement

is significant. This method can also be applied to various applications that require centimeter accuracy.

Data availability All of the data, models, and codes that support the findings of this study are available. Multi-GNSS orbit and clock products are available online for free (https://cddis.nasa.gov/archive/gnss/products/mgex/1982/). The RINEX observations used in this study and the codes for variance components estimation of the code and phase observations in the PPP method were prepared by the authors and are available from the corresponding author by request.

Declarations

Conflict of interest The authors declare no conflict of interest.

References

Abou-Galala M, Rabah M, Kaloop M, Zidan ZM (2018) Assessment of the accuracy and convergence period of precise point positioning. Alex Eng J 57(3):1721–1726

Afifi A, El-Rabbany A (2013) Stochastic modeling of Galileo E1 and E5a signals. International Journal of Engineering and Innovative Technology (IJEIT) 3(6):188–192

Alcay S, Ogutcu S, Kalayci I, Yigit CO (2019) Displacement monitoring performance of relative positioning and Precise Point Positioning (PPP) methods using simulation apparatus. Adv Space Res 63(5):1697–1707

Amiri-Simkooei A (2007) Least-squares variance component estimation: theory and GPS applications. Delft University of Technology, Delft

Amiri-Simkooei AR, Teunissen PJG, Tiberius CCJM (2009) Application of least-squares variance component estimation to GPS observables. J Surv Eng 135(4):149–160

Amiri-Simkooei AR, Asgari J, Zangeneh-Nejad F, Zaminpardaz S (2012) Basic concepts of optimization and design of geodetic networks. J Surv Eng 138(4):172–183

Amiri-Simkooei AR (2013) Application of least squares variance component estimation to errors-in-variables models. J Geodesy 87(10–12):935–944

Amiri-Simkooei AR, Zangeneh-Nejad F, Asgari J (2013) Least-squares variance component estimation applied to GPS geometry-based observation model. J Surv Eng 139(4):176–187

Amiri-Simkooei AR, Alaei-Tabatabaei SM, Zangeneh-Nejad F, Voosoghi B (2017) Stability analysis of deformation-monitoring network points using simultaneous observation adjustment of two epochs. J Surv Eng 143(1):04016020

Avallone A, Marzario M, Cirella A, Piatanesi A, Rovelli A, Di Alessandro C, D'Anastasio E, D'Agostino N, Giuliani R, Mattone M (2011) Very high rate (10 Hz) GPS seismology for moderate-magnitude earthquakes: the case of the Mw 6.3 L'Aquila (central Italy) event. J Geophys Res: Solid Earth 116(B2)

Beran T (2008) Single-frequency, single receiver terrestrial and spaceborne point positioning

Bisnath S, Gao Y (2009) Current state of precise point positioning and future prospects and limitations. In Observing our changing earth (pp. 615–623). Springer: Berlin

Böhm J, Niell A, Tregoning P, Schuh H (2006) Global mapping function (GMF): a new empirical mapping function based on numerical weather model data. Geophys Res Lett 33(7)

Bona P (2000) Precision, cross correlation, and time correlation of GPS phase and code observations. GPS Solutions 4(2):3–13

Cai C, Gao Y (2013) Modeling and assessment of combined GPS/GLONASS precise point positioning. GPS Solutions 17(2):223–236

Cai C, Gao Y, Pan L, Zhu J (2015) Precise point positioning with quad-constellations: GPS, BeiDou, GLONASS and Galileo. Adv Space Res 56(1):133–143

Capilla RM, Berné JL, Martín A, Rodrigo R (2016) Simulation case study of deformations and landslides using real-time GNSS precise point positioning technique. Geomat Nat Haz Risk 7(6):1856–1873

Chatterjee RS, Thapa S, Singh KB, Varunakumar G, Raju EVR (2015) Detecting, mapping and monitoring of land subsidence in Jharia Coalfield, Jharkhand, India by spaceborne differential interferometric SAR, GPS and precision levelling techniques. J Earth Syst Sci 124(6):1359–1376

Dabove P, Manzino AM, Taglioretti C (2014) GNSS network products for post-processing positioning: limitations and peculiarities. Applied Geomatics 6(1):27–36

Dabove P, Linty N, Dovis F (2020) Analysis of multi-constellation GNSS PPP solutions under phase scintillations at high latitudes. Applied Geomatics 12(1):45–52

Eueler HJ, Goad CC (1991) On optimal filtering of GPS dual frequency observations without using orbit information. Bulletin Géodésique 65(2):130–143

Erol S, Erol B, Ayan T (2004) A general review of the deformation monitoring techniques and a case study: analysing deformations using GPS/levelling. In XXth ISPRS Congress (pp. 12–23)

Erol S, Ayan T (2003) An investigation on deformation measurements of engineering structures with GPS and levelling data: case study. In International Symposium on "Modern Technologies, Education and Professional Practice in the Globalizing World", Sofia

Fermi A, Realini E, Venuti G (2019) The impact of relative and absolute GNSS positioning strategies on estimated coordinates and ZWD in the framework of meteorological applications. Applied Geomatics 11(1):25–38

Fund F, Perosanz F, Testut L, Loyer S (2013) An integer precise point positioning technique for sea surface observations using a GPS buoy. Advances in Space Research 51(8):1311–1322

Gandolfi S, Tavasci L, Poluzzi L (2017) Study on GPS–PPP precision for short observation sessions. GPS Solutions 21(3):887–896

Gao C, Wu F, Chen W, Wang W (2011) An improved weight stochastic model in GPS Precise Point Positioning. In Proceedings 2011 International Conference on Transportation, Mechanical, and Electrical Engineering (TMEE) (pp. 629–632). IEEE

Ge M, Gendt G, Rothacher MA, Shi C, Liu J (2008) Resolution of GPS carrier-phase ambiguities in precise point positioning (PPP) with daily observations. J Geodesy 82(7):389–399

Guo J, Geng J, Wang C (2021) Impact of the third frequency GNSS pseudorange and carrier phase observations on rapid PPP convergences. GPS Solutions 25(2):1–12

Geng J, Jiang P, Liu J (2017) Integrating GPS with GLONASS for high-rate seismogeodesy. Geophys Res Lett 44(7):3139–3146

Gerdan GP (1995) A comparison of four methods of weighting double difference pseudorange measurements. Australian Surveyor 40(4):60–66

Hadas T, Hobiger T, Hordyniec P (2020) Considering different recent advancements in GNSS on real-time zenith troposphere estimates. GPS Solutions 24(4):1–14

Hammond WC, Thatcher W (2005) Northwest Basin and Range tectonic deformation observed with the Global Positioning System, 1999–2003. J Geophys Res: Solid Earth 110(B10)

Han S (1997) Quality-control issues relating to instantaneous ambiguity resolution for real-time GPS kinematic positioning. J Geodesy 71(6):351–361

Helmert FR (1907) Die Ausgleichungsrechnung nach der Methode der kleinsten Quadrate: mit Anwendungen auf die Geodàsie, die Physik und die Theorie der Messinstrumente. BG Teubner

Héroux P, Gao Y, Kouba J, Lahaye F, Mireault Y, Collins P, Macleod K, Tétreault P, Chen K (2004) Products and applications for precise point positioning-moving towards real-time. In Proceedings of the 17th international technical meeting of the satellite division of The Institute of Navigation (ION GNSS 2004) (pp. 1832–1843)

Hofmann-Wellenhof B, Lichtenegger H, Wasle E (2007) GNSS–global navigation satellite systems: GPS, GLONASS, Galileo, and more. Springer Science & Business Media

Hu H, Gao J, Yao Y (2014) Land deformation monitoring in mining area with PPP-AR. Int J Min Sci Technol 24(2):207–212

Jin XX, de Jong CD (1996) Relationship between satellite elevation and precision of GPS code observations. The Journal of Navigation 49(2):253–265

Kalkan Y, Potts LV, Bilgi S (2016) Assessment of vertical deformation of the atatürk dam using geodetic observations. J Surv Eng 142(2):04015011

Karimi H (2021) An analysis of satellite visibility and single point positioning with GPS, GLONASS, Galileo, and BeiDou-2/3. Appl Geomatics, pp.1–11

Koch KR (1999) Parameter estimation and hypothesis testing in linear models. Springer

Kouba J, Héroux P (2001) Precise point positioning using IGS orbit and clock products. GPS Solutions 5(2):12–28

Kouba J, Lahaye F, Tétreault P (2017) Precise point positioning. In Springer Handbook of Global Navigation Satellite Systems (pp. 723–751). Springer: Cham

Larson KM (2009) GPS seismology. J Geodesy 83(3–4):227–233

Li X, Li X, Yuan Y, Zhang K, Zhang X, Wickert J (2018) Multi-GNSS phase delay estimation and PPP ambiguity resolution: GPS, BDS, GLONASS, Galileo. J Geodesy 92(6):579–608

Li G, Geng J (2019) Characteristics of raw multi-GNSS measurement error from Google Android smart devices. GPS Solutions 23(3):1–16

Li B, Lou L, Shen Y (2016) GNSS elevation-dependent stochastic modeling and its impacts on the statistic testing. J Surv Eng 142(2):04015012

Li B (2016) Stochastic modeling of triple-frequency BeiDou signals: estimation, assessment and impact analysis. J Geodesy 90(7):593–610

Li B, Shen Y, Xu P (2008) Assessment of stochastic models for GPS measurements with different types of receivers. Chin Sci Bull 53(20):3219–3225

Li B, Shen Y, Lou L (2010) Efficient estimation of variance and covariance components: a case study for GPS stochastic model evaluation. IEEE Trans Geosci Remote Sens 49(1):203–210

Li X, Zhang X (2012) Improving the estimation of uncalibrated fractional phase offsets for PPP ambiguity resolution. The Journal of Navigation 65(3):513–529

Lou Y, Zhang W, Wang C, Yao X, Shi C, Liu J (2014) The impact of orbital errors on the estimation of satellite clock errors and PPP. Adv Space Res 54(8):1571–1580

Luo X, Mayer M, Heck B, Awange JL (2014) A realistic and easy-to-implement weighting model for GPS phase observations. IEEE Trans Geosci Remote Sens 52(10):6110–6118

Martín A, Anquela AB, Dimas-Pagés A, Cos-Gayón F (2015) Validation of performance of real-time kinematic PPP. A possible tool for deformation monitoring. Measurement 69:95–108

Marreiros JPR, Bastos MLMC, Fernandes MJAP (2012) Kinematic GNSS precise point positioning: application to marine platforms. FCUP

Melbourne W (1985) The case for ranging in GPS-based geodetic systems. In Proc. 1st int. symp. on precise positioning with GPS (pp. 373–386)

Nickitopoulou A, Protopsalti K, Stiros S (2006) Monitoring dynamic and quasi-static deformations of large flexible engineering structures with GPS: accuracy, limitations and promises. Eng Struct 28(10):1471–1482

Parvazi K, Farzaneh S, Safari A (2020) Role of the RLS-VCE-estimated stochastic model for improvement of accuracy and convergence time in multi-GNSS precise point positioning. Measurement 165:108073

Paziewski J, Sieradzki R, Baryla R (2018) Multi-GNSS high-rate RTK, PPP and novel direct phase observation processing method: application to precise dynamic displacement detection. Measurement Science and Technology 29(3):035002

Poluzzi L, Tavasci L, Corsini F, Barbarella M, Gandolfi S (2020) Low-cost GNSS sensors for monitoring applications. Applied Geomatics 12(1):35–44

Prokopov A, Matvienko S, Meleshko A, Serkina T, Androsov M (2009) Relativistic effects in global satellite navigation systems. Acta Astronaut 64(1):67–74

Qian K, Wang J, Hu B (2016) A posteriori estimation of stochastic model for multi-sensor integrated inertial kinematic positioning and navigation on basis of variance component estimation. The Journal of Global Positioning Systems 14(1):5

Quan Y, Lau L, Roberts GW, Meng X (2016) Measurement signal quality assessment on all available and new signals of multi-GNSS (GPS, GLONASS, Galileo, BDS, and QZSS) with real data. The Journal of Navigation 69(2):313–334

Rebeyrol E, Julien O, Macabiau C, Ries L, Delatour A, Lestarquit L (2007) Galileo civil signal modulations. GPS Solutions 11(3):159–171

Roberts GW, Tang X, Brown CJ (2019) Measurement and correlation of displacements on the Severn Suspension Bridge using GPS. Applied Geomatics 11(2):161–176

Savage JC, Gan W, Prescott WH, Svarc JL (2004) Strain accumulation across the Coast Ranges at the latitude of San Francisco, 1994–2000. J Geophys Res: Solid Earth 109(B3)

Savšek-Safić S, Ambrožič T, Stopar B, Turk G (2006) Determination of point displacements in the geodetic network. J Surv Eng 132(2):58–63

Tang X, Roberts GW, Li X, Hancock CM (2017) Real-time kinematic PPP GPS for structure monitoring applied on the Severn Suspension Bridge. UK, Advances in Space Research 60:925–937

Teunissen PJG (1988) Towards a least-squares framework for adjusting and testing of both functional and stochastic model. Internal Research Memo, Delft Geodetic Computing Centre, Dept. of Geodetic Engineering, Delft Univ. Of Technology, Delft, Netherlands

Vodopivec F, Savsek-Safic S (2003) Determination of stable points in deformation analysis. In EGS-AGU-EUG Joint Assembly (p. 3621).

Wang J, Satirapod C, Rizos C (2002) Stochastic assessment of GPS carrier phase measurements for precise static relative positioning. J Geodesy 76(2):95–104

Wu JT, Wu SC, Hajj GA, Bertiger WI, Lichten SM (1992) Effects of antenna orientation on GPS carrier phase. Astrodynamics 1991:1647–1660

Xu CH, Wang JL, Gao JX, Jian WANG, Hong HU (2011) Precise point positioning and its application in mining deformation monitoring. Transactions of Nonferrous Metals Society of China 21:s499–s505

Yigit CO, Coskun MZ, Yavasoglu H, Arslan A, Kalkan Y (2016) The potential of GPS precise point positioning method for point displacement monitoring: a case study. Measurement 91:398–404

Yigit CO (2016) Experimental assessment of post-processed kinematic precise point positioning method for structural health monitoring. Geomat Nat Haz Risk 7(1):360–383

Yu J, Meng X, Shao X, Yan B, Yang L (2014) Identification of dynamic displacements and modal frequencies of a medium-span suspension bridge using multimode GNSS processing. Eng Struct 81:432–443

Zangeneh-Nejad F, Amiri-Simkooei AR, Sharifi MA, Asgari J (2015) On the realistic stochastic model of GPS observables: implementation and performance. Int Arch Photogramm, Remote Sens Spatial Inform Sci 40

Zangeneh-Nejad F, Amiri-Simkooei AR, Sharifi MA, Asgari J (2017) Recursive Least Squares with real time stochastic modeling: application to GPS relative positioning. Int Arch Photogramm, Remote Sens Spatial Inform Sci 42

Zangeneh-Nejad F, Amiri-Simkooei AR, Sharifi MA, Asgari J (2018) Recursive least squares with additive parameters: application to precise point positioning. J Surv Eng 144(4):04018006